

## SUBSTORM RECOVERY PHASE: RELATIONSHIP TO NEXT ACTIVATION

R.J. Pellinen<sup>1</sup>, H.J. Opgenoorth<sup>2</sup>, T.I. Pulkkinen<sup>1</sup><sup>1</sup>Finnish Meteorological Institute, Box 503, SF-00101, Helsinki, Finland<sup>2</sup>Swedish Institute of Space Physics, Uppsala division, S-75591 Uppsala, Sweden

## ABSTRACT

In this work, the relationship of the substorm recovery and simultaneous growth of new substorm activity is discussed using satellite imaging and ground-based ionospheric observations. We present examples where omegabands are observed in the poleward edge of the diffuse morning sector auroral oval during the later phase of the substorm recovery, simultaneously with generation of new activity in the evening sector. It appears that the recovery-phase associated precipitation is considerably harder than the evening-sector precipitation associated with the substorm expansion phase. Furthermore, the strong increase in both intensity and energy of the morning-side precipitation suggests a new type of activity in that local time sector, not only a decay of the pre-existing ionospheric current system. To actually separate the new activation and the recovery of the previous substorms, magnetograms from three longitudinal chains separated by several hours in local time have been investigated. The new activation is in each case triggered in the region where the peak activity of the previous substorm was located.

propagation of the westward travelling surge into the evening sector (Ref.2). At the end of the substorm expansion phase the growth of the auroral bulge stops and the substorm current wedge starts to decay. During the recovery phase, the auroral intensity decreases and the most intense precipitation is observed in the morning sector. The ongoing activity in the morning side generates the long tail often observed in the AL index.

During the recovery phase, the precipitation into the morning sector intensifies along the sharp poleward boundary that later develops into a wavy curtain-type structures, the so-called omega bands. These structures, although not always observed in connection with recovery phases, are typical signatures of the later phase of the substorm recovery, which we identify from the AE index as the slower decay towards a quiet-time value (Ref.3). Simultaneously, discrete forms often appear further poleward, separated by about ten degrees in latitude from the wavy boundary. These structures often connect to the oval only at their western edge.

## 1. INTRODUCTION

Recent possibilities to study the magnetospheric substorm in a global sense using multipoint satellite measurements, extensive ground-based networks, and global satellite imaging have revealed that the substorm sequence also involves changes in the local time sector of the peak activity. During the growth phase the ionospheric current system is enhanced and moves equatorward as a consequence of energy loading into the magnetospheric tail (Ref.1). The substorm expansive phase is characterized by the poleward expansion of the auroras and the

In a recent study utilizing Viking imager data and previously published auroral observations of omega-bands, we concluded that in all the cases studied, the omega-bands appeared at relatively low magnetic latitudes during the later phase of the recovery phase (Ref.3). Magnetic field-aligned mapping located the source regions of these omega-bands to the near-Earth magnetotail close to the geostationary distance. However, the topological connection of the high-latitude precipitation into the magnetotail remains unclear; a source within the plasma sheet boundary layer has been suggested by Craven and

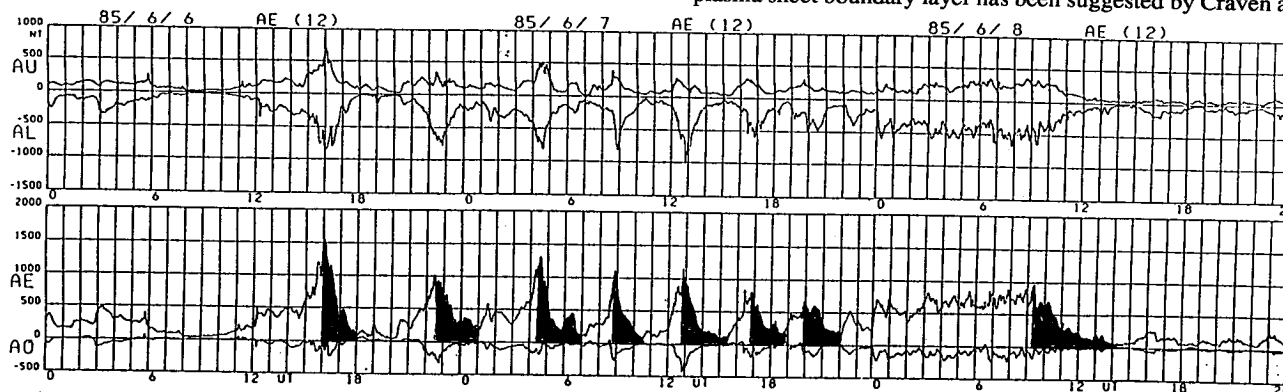


Fig.1 AU, AL, and AE indices from June 6-8, 1985. The recovery phases of different substorm periods are indicated by shaded areas.

Frank (Ref.4). Clearly, a better understanding of the magnetic field development in the near-Earth tail during the later phases of the substorm is needed in order to resolve this issue.

Opgenoorth et al. (Ref.5) studied the auroral signatures of the recovery phase using radar data combined with other ground-based measurements and satellite images. They further confirmed that the morning-sector precipitation is considerably harder than that in the evening sector, and that this hard precipitation is particularly associated with the substorm recovery phase. Persson et al. (Ref.6) found that there are significant changes in the ionospheric conductivities: In the evening sector and during the expansion phase both the Hall and the Pedersen conductivities increase with increased particle precipitation. However, due to the additional high energy precipitation the Hall conductivity increases faster, which results in a ratio of Hall to Pedersen conductivity ( $\sigma_H/\sigma_P$ ) larger than 3. In the morning sector and during substorm recovery the precipitation can be so energetic that only the Hall conductivity is enhanced, while the Pedersen conductivity can decrease as compared to the value in the evening sector. Again, the resulting Hall to Pedersen ratio is very high. Due to the low Pedersen conductivity and a low altitude Hall conductivity maximum the ionosphere-magnetosphere coupling has to be quite different from the extensively studied processes in the evening sector discrete aurora. The intensity of the precipitation and the lack of any significant parallel acceleration in the particle data (Ref.7) suggests that a new mechanism is activated for precipitation of the particles in the morning-sector near-Earth magnetotail during the late recovery phase.

The high-energy precipitation maps into the magnetotail near the outer boundary of the ring current close to the geostationary orbit. This suggests an adiabatic acceleration mechanism which involves pitch angle scattering of trapped particles into the loss cone. A less dramatic final dipolarization of the magnetosphere might be able to account for the observations described above (see Ref.5 for further discussion). This process occurs during the period when the plasma sheet expands in the mid-tail region, and the near-Earth neutral line retreats tailward, as has been suggested by Hones et al. (Ref.8). The geostationary signatures of the recovery phase associated precipitation is left for a future study.

Toward the end of the recovery phase, a new substorm expansion may start in the evening sector, without any spatial connection to the recovery phase region either in the ionosphere or in the magnetotail. Preliminary examination of the geostationary orbit data suggests that while the recovery phase signatures are clearly observable in the ionosphere, simultaneously a new growth phase may be in progress in the magnetotail, characterized by energy loading into the magnetosphere and consequent stretching of the near-Earth tail field. However, signatures typical of the growth phase development are not always seen in the auroral electrojet indices preceding these expansion onsets. Therefore, we have investigated in detail the local magnetograms from evening, midnight, and morning sectors, covering the latitudinal range extending across the discrete auroral oval. This allows us to draw conclusions about the differences in the recovery phase development in the different local time sectors.

## 2. OBSERVATIONS

### 2.1 Recovery phase characteristics based on AE indices

Regularly published AE (AL and AU) indices are commonly used as quick-look information for magnetospheric and ionospheric substorm activity. An experienced scientist can easily distinguish between different substorm phases in the data. In clear-cut cases, the substorm expansion onset moment is well identified. Also, in most of the cases, the growth phase signatures are easily recognized. However, the moment of the recovery phase onset is harder to resolve, mainly due to the large variety of current components existing in different time sectors of the auroral oval. Hence, AE data should only be used for conclusions and rough estimates on average substorm development, and more detailed studies should include investigation of individual auroral zone magnetograms in order to separate between temporal and spatial effects in the entire auroral oval.

Fig. 1 gives an example of a typical AE, AU, AL presentation covering a period of 72 hours. During this time interval 7 more or less clear substorm activations can be identified. The whole sequence of substorms ends in a so-called steady magnetospheric convection period (Sergeev et al., Ref.9) lasting for about 16 hours and having a continuous disturbance level of more than 500 nT. The recovery phases of different substorm periods are indicated by shaded areas. The shortest substorm period is of the order of 3 hours.

Fig.2 shows a typical AE index behaviour and the associated auroral development during an idealized substorm. We assume

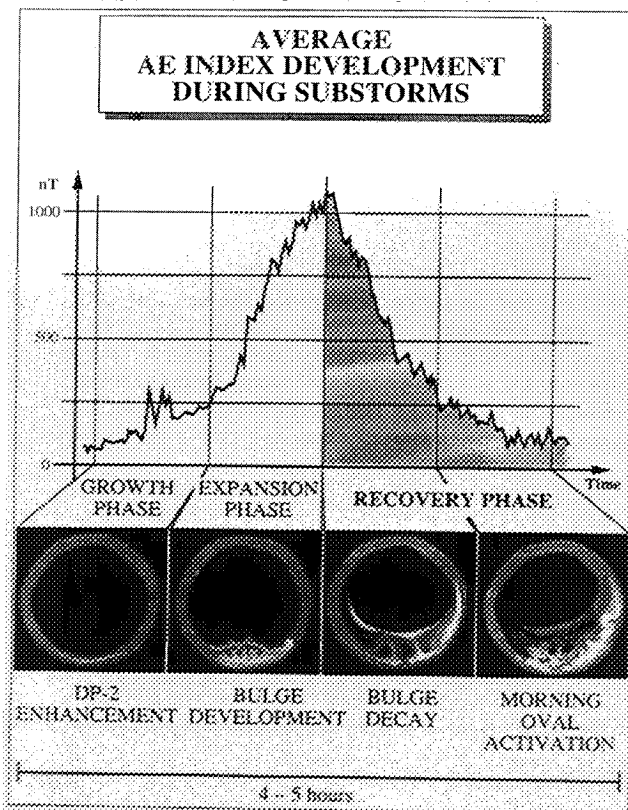


Fig.2 Typical AE index behaviour and the auroral oval development during an idealized substorm.

that the recovery phase starts after the AE maximum has been reached and when the current system starts to decay, which is indicated by the steep negative derivative of the AE curve and ends when the absolute minimum has been reached. The length of the recovery phase is, in average, about 2 hours. In the AE index we can distinguish two different types of behaviour during the recovery, steep drop (bulge decay) followed by a more smooth decrease (morning oval activation) dividing the recovery period into two intervals almost equal in time.

Another point we would like to rise is the coincidence of the AU maxima and AL minima in all the cases (Fig.1). In most of the events the AL maxima are slightly delayed. It is difficult to say whether this is a temporal effect or whether it is barely due to a latitudinal asymmetry of the current systems. However, the coincidence demonstrates that both in the evening sector and in the morning sector the current system decay takes place in parallel. In the evening side, the decay may be smoothened due to an onset of a new growth phase in this time sector.

In Fig.1 we presented a more or less ideal case where the separations between different substorms were quite evident and easy to identify. In Fig.3 we show a more complicated case

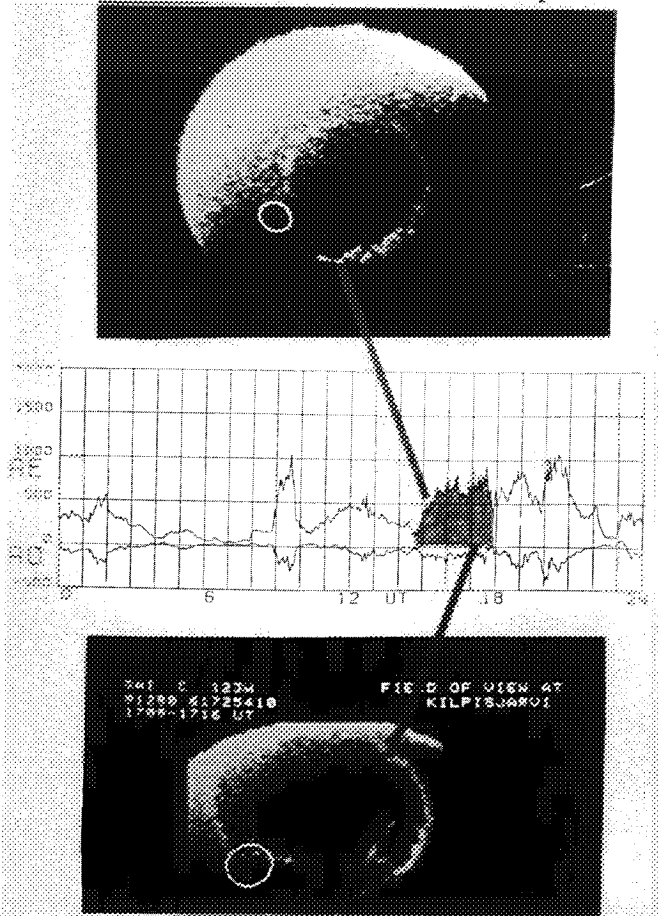


Fig.3 Auroral oval development during a more complicated substorm. The upper panel shows the auroral situation 30 min after break-up and the lowest panel the recovery phase two hours later about 30 min before the new activation. All-sky camera field of view at Kilpisjärvi, Finland, is indicated by the ring. (DE-1 images: Courtesy by L. Frank and J. Craven).

where also some characteristic auroral oval features are demonstrated using DE-1 UV images. The substorm starts at about 1440 UT, and about 30 min later the bulge covers a substantial part of the nightside auroral oval (upper panel). Two hours later the expansion has obviously stopped and the whole oval shows characteristic signatures of late recovery phase aurora: weakening irregular structures in the evening sector, weakly illuminated wide oval in the midnight sector and bright morningside oval with wavy poleward boundary and a poleward discrete arc-type structure separated by a dark gap of about 10 degrees in latitude from the equatorward bright area (lower panel). The AU-AL curves in the middle panel show that the obvious recovery phase does not lead to a quiet situation but a new activation follows immediately around 1750 UT (35 min after the auroral conditions presented in the lower panel) when the AL is about 200 nT and AE about 450 nT.

A common feature in all the cases presented above is that each obvious recovery phase case is almost immediately followed by a new activation. In Figs.1 and 2 growth phase signatures (enhanced convection, DP-2 type current development) were observed before each activation while in Fig.3 growth phase signatures are less evident due to the high level of initial activity. In Fig.4 we demonstrate a case which is quite different from the two previous ones: The AE index stays on a quiet level for more than 20 hours and continues to be quiet for over 10 hours after a highly localized substorm in a narrow local time sector around midnight. The substorm itself seems to be highly correlated with the IMF variations. In this case, the AU index reaches its maximum during the late recovery phase and the auroral oval in the DE-1 images (data not shown) is covered with wide diffuse precipitation without any definite discrete structures like in the previous case. There is also a clear evening-morning asymmetry, the precipitation into the morningside being over much wider range of latitudes than that into the eveningside.

## 2.2 Analysis based on oval images and individual magnetograms

During the last two decades, satellite-borne auroral imaging has provided further details on auroral behaviour during different substorm phases. As shown above, recovery phase auroras are not localized but appear in a wide range of longitudes along the morningside auroral oval. Their temporal behaviour after (and during) expansion phase is of great interest. To study the development in detail, a sufficiently high imaging resolution, both time and space, is required. The Swedish Viking satellite mission carried out in 1986 was the first one to offer such an

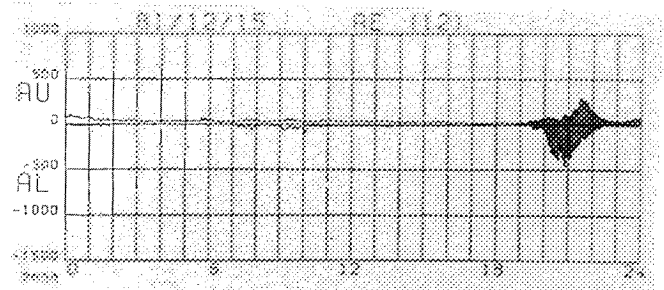


Fig.4 Isolated IMF-controlled AE substorm event preceded by 20 and followed by 10 hours quiet period.

opportunity (Ref.10). Below we present two separate cases where the auroral development along the auroral oval is documented by the Viking imaging data. Supporting ground-based data were collected in a coordinated manner, which gives additional information on the ionospheric electrodynamic development during the substorm recovery.

Fig.5 shows the global development of auroral activity from the decay of the expansion phase auroral fragments (upper panels) to the near end of the recovery phase (lower panels). Details of the substorm are given in Pulkkinen et al. (Ref.3). The first Viking image taken on March 25, 1986 at 2046:53 UT, 47 min after the substorm onset ( $T=+47$ ), shows a stationary surge over Greenland that has started to decay. The disintegration seems to last for about 15 min. Simultaneously, diffuse auroral structures limited by a wavy poleward boundary over Svalbard (with some local magnetic effects at Ny Alesund, Svalbard, data not shown) appear further to the east, as shown in the first frame on the second row. At 2119 UT,  $T=+80$ , (last frame on third row) the surge has disappeared and the activity has transferred to the east with a bright poleward structure appearing in the premidnight sector. Twenty minutes later, at

about 2130 UT, the auroral activity to the west has subsided while along the Siberian coast two hook-type active forms appear. These hooks are UV signatures of auroral omega bands (Ref.11) moving eastward along the morningside auroral oval. The last panel in Fig.5 shows that almost all auroral activity is in the eastern sector near the end of the recovery phase. The hooks appear during this stage and remain visible for about 20-30 min, becoming gradually more unstructured and obviously finally merging with the bright auroras along the morningside oval.

Global magnetic data from auroral latitude stations are presented in Fig.6. Overlaid in the figure is a schematic drawing of the auroral hooks as recorded by Viking at 2141 UT (the original image shown in the lower right corner). Also the AU and AL curves are included in Fig.6. Around 2100 UT when the surge was in the decaying mode over Greenland magnetic activity was rapidly decreasing in this time sector. In the east, from Scandinavia to the Siberian stations, a more gradual decay of magnetic activity is evident obviously due to the transfer of precipitation activity to these regions during the recovery phase. The same effect is also visible in the AL index

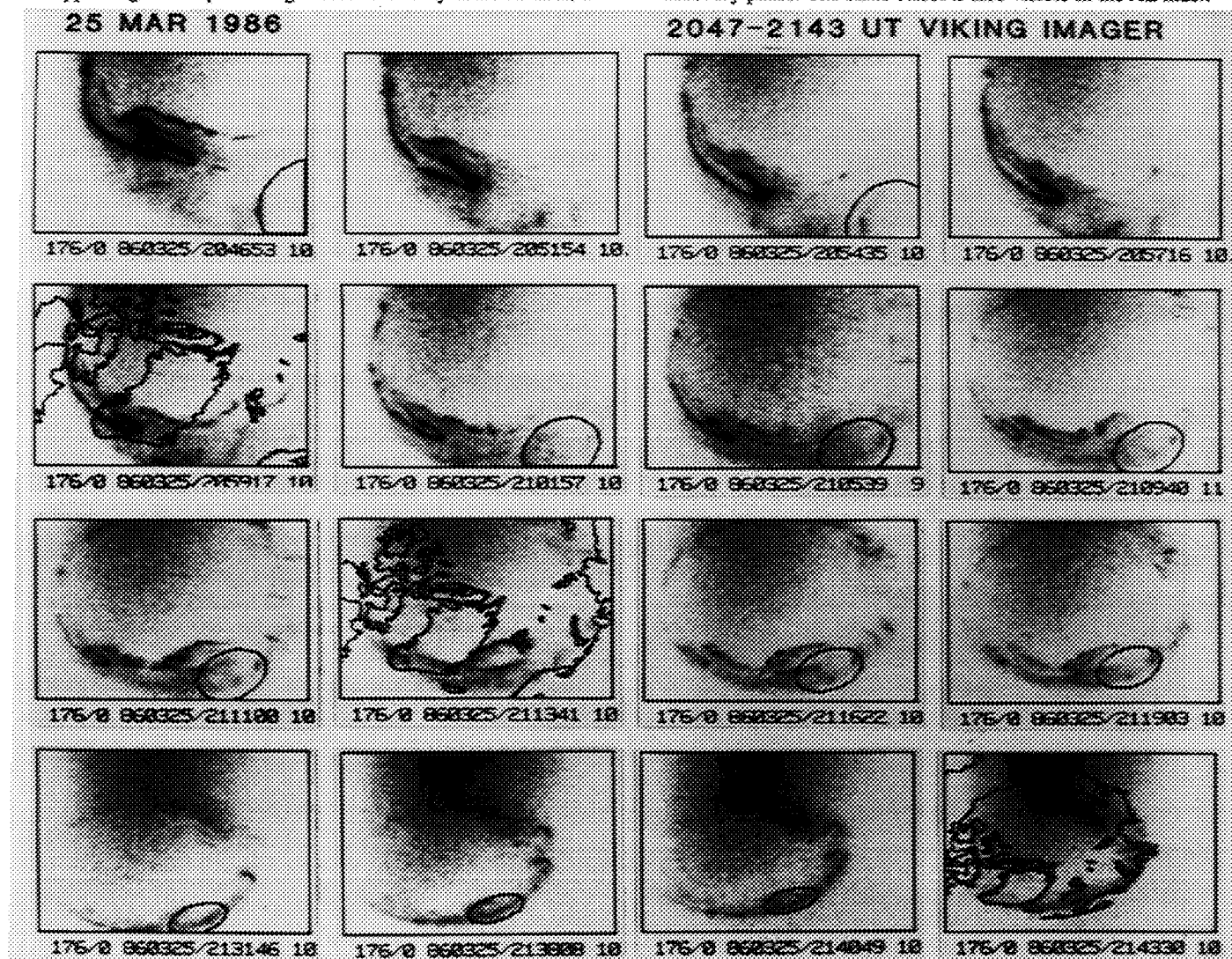


Fig.5 Development of auroral activity on Mar 25, 1986 from 2047 to 2143 UT recorded by the Viking satellite imager.

where the gradual recovery reflects the prolonged depression of the magnetic H-component in the morning sector.

A new activation starts slightly after 2200 UT in the Greenland and Iceland local time sector. Both AU and AL indices are abruptly disturbed, and the AE level is near 1000 nT. The auroral activity of the previous recovery phase is at this time in the late morning sector, whereas the new activation takes place in the evening sector at almost opposite side of the oval (about 8-10 hours shift in time). In Fig.6 the southernmost Canadian stations show mainly eastward electrojet effects disturbed by the current wedge expanding to Baker Lake (BLC), which indicates that a surge was formed in the Greenland sector and propagated westward. The activation expands clearly eastward reaching the longitude of the preceding recovery phase expansion.

In Fig.6 the most dramatic drop in magnetic field appears at Leirvogur (LRV), Iceland starting at about 2210 UT. During the preceding 30 min (i.e., during the recovery phase activity in the morning sector) the magnetic field is gradually decreasing by about 110 nT. The two southernmost stations in Greenland (NAQ, FHB) indicate a similar type of trend and, obviously, NAQ is the first station to be activated after which the activity spreads (mainly) toward north and east. The meridional data from Greenland suggests that a Harang discontinuity-type development might have occurred in that time sector just before the onset.

It is interesting to note that the activity starts in the same area where the surge of the previous activity had some 80 min earlier stopped and decayed. It is also worthwhile to observe that the new activity appears to be spreading more eastward into the region where the previous activity was operating. From the Viking image in Fig.6 we can see that there is a quiet arc with a localized bright spot developing in the evening sector over Iceland. 30 min later a new substorm breaks up in this region. Based on these facts it may be concluded that some kind of growth phase activity takes place in the evening sector meanwhile the omega bands are visible in the late morning sector.

Fig 7. introduces another case with omega bands developing towards the end of the recovery phase. In this case Finland is in the morning sector (4 hours after midnight) and the omega bands are visible also in the ASC data from Finland. In both cases (Figs. 6 and 7) the AE indices show about two hours of recovery with similarities in the shapes of AL indices during the recovery phases. The only striking difference is in the steepness of the following activation, in this case the enhancement of the AE index is more gradual. Also the preceding activity has some similarities with the previous example. A substorm which started in the Scandinavian sector at about 2200 UT was preceded by a growth phase for 60 min (Ref.12) and it was followed by a new activation in the Greenland-Scandinavia sector at about 2300 UT. During this activation the AE index reached 1000 nT level. The recovery phase started slightly after 2400 UT and it is quite evident that the auroral

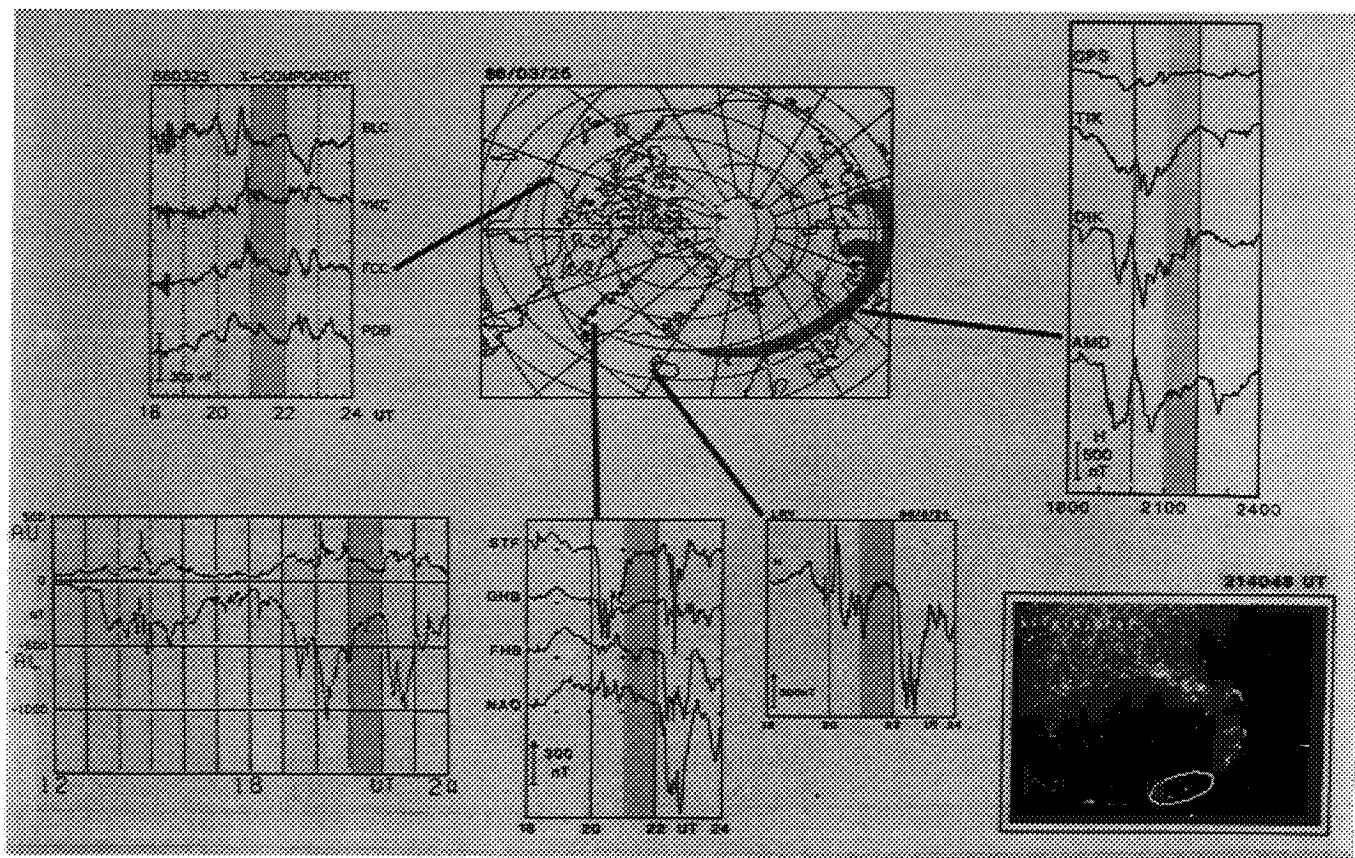


Fig.6 Global magnetic data from three different time sectors. Auroral structures shown on the image are overlaid on the map. The later phase of substorm recovery is indicated by shading in the magnetograms and in the AU, AL curves.



activity was gradually shifted to the morning sector to about 8 hours to the east of the Greenland sector.

The Greenland stations between GHB and ATU show a very steep recovery starting at about 0030 UT and reaching nearly quiet level at about 0100 UT. A local activation starts at 0120 UT at GHB and propagates poleward and westward to be seen at PDB in the Canadian sector. This activation is simultaneous to the appearance of the omega bands in the Scandinavian sector, which produce a characteristic local magnetic disturbance as seen in the EISCAT magnetometer cross and STARE data (data not shown). The activation ceases at about 0200 UT, and is followed by a new more impulsive activation in the Greenland sector some 15-20 min later. This activation leads to new substorm development also recorded by the AE index.

This event, as the previous one, presents some evidence that new substorm activity is about to develop in the evening sector when omega bands appear in the morning sector some 6-8 hours away. The new activity develops in the region where the peak activity was recorded some 100 min earlier. In this case we do not see only growth a phase type development, but also a local small activation resembling a "pseudobreakup" (Ref.13). This activation is not clearly visible in the AE index because it appears on higher latitudes than the typical AE stations while the main activity itself takes place further equatorward and affects the AE index.

### 3. DISCUSSION AND CONCLUSIONS

We have presented detailed data from several substorm sequences where it becomes evident that the recovery phase disturbance is not just a decay from the previous disturbance level until a new substorm disturbance initiates. There are clearly two distinct phases in the substorm recovery. It appears that the large-scale morning sector auroral forms (known as omega bands) appear only for 20-30 minutes in the second phase of recovery. During multiple substorm sequences the appearance of omega bands in the morning sector is associated with a simultaneous new activation of the evening sector, which indicates that different substorm phases can simultaneously be under progress in different local time sectors. Future studies of recovery phase phenomena should therefore carefully make use of simultaneous local observations in the different local time zones. The global AE index alone cannot resolve such complicated development.

In this context it is interesting to note that the new evening sector activity starts 8-10 hours away from the omega band region, in the same area where the previous expansion phase features have just decayed. This observation might indicate that the region of the magnetotail where the previous energy release terminated is the region which grows first unstable after a renewed magnetospheric energy storage. One possible explanation might be an effective tail-like deformation of the near-Earth eveningside magnetic field due to the injection of fresh current-carrying ions into these regions during the recovery

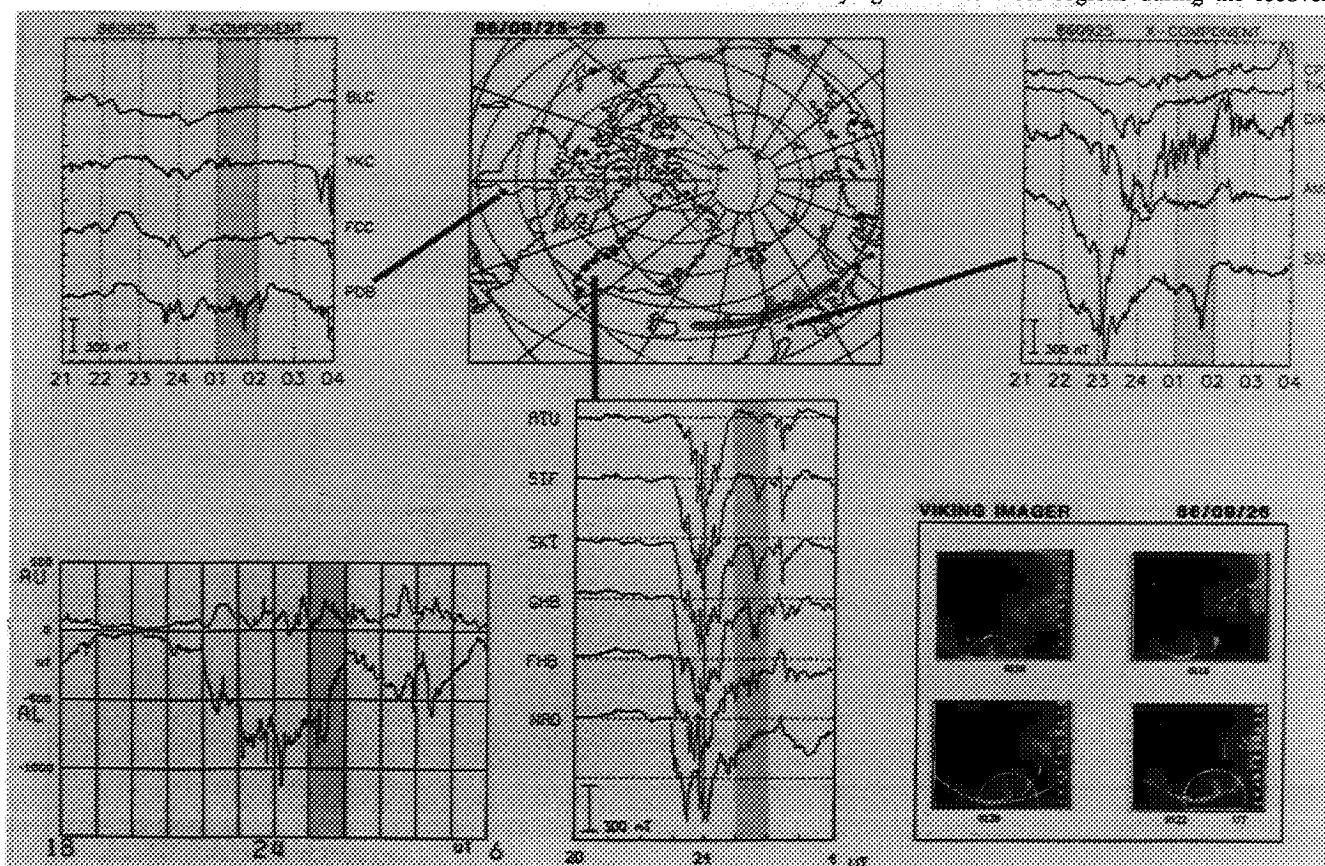


Fig.7 Similar to Fig. 6. The auroral structure on the map corresponds to the 0120 UT frame. The dots on the map give the locations of the magnetic recording sites.

phase.

In this paper we have mainly dealt with recovery phases followed by a new intensification. However, there are cases where isolated substorms develop into omega bands in the morning sector without leading to a new substorm intensification (e.g. Ref.14). The morning sector processes lead in all cases into eastward expanding diffuse aurora that seem to be close to an instability. Omega bands do develop even during isolated substorms, but definitely omega bands will appear if a new intensification starts. A new growth phase will add to the field-aligned current flow in both morning and evening sectors. If the morning sector is close to instability because of the on-going recovery phase, a new additional growth phase current increase may trigger the instability, and omega bands will appear.

As is typical for substorm studies, our new detailed data from recovery phases of multiple substorm sequences have raised a number of new questions. The first obvious question deals with the IMF correlation. Are the new activations of substorm-type energy release triggered by changes in the IMF, or are the processes due to a recurrent release of stored magnetospheric energy in a situation of stable solar wind energy input?

The second question deals with the ionospheric control. What role does the ionosphere and neutral atmosphere play in "delaying" the substorm recovery, or are they even actively involved in the enhancement of the morning sector disturbances? The different altitude distribution of ionospheric conductivities might play an important role in the processes described above. Also the differences in ionospheric Pedersen conductivities in the evening (high) and morning (low) sectors might favour an onset of field-aligned substorm currents in the evening sector (and the associated magnetosphere-ionosphere coupling) as pointed out by Pellinen (Ref.15).

The third question is related with electron acceleration. Where do the injected electrons go and are they adiabatically accelerated during substorm recovery phase? Why is the precipitation asymmetric being of high energy in the morning sector and (probably) more dispersed and of lower energy in the evening-premidnight sector.

We shall continue our work on recovery phase phenomena, with particular concentration on simultaneous local observations in different local time sectors in the ionosphere, and also in the magnetosphere at geostationary orbit. As mentioned earlier, the mapping of the discussed phenomena to the near-Earth equatorial region indicates that geostationary satellite data could add new information to the questions raised by this and earlier studies dealing with recovery phase phenomena.

#### 4. ACKNOWLEDGEMENTS

We are grateful to E. Friis-Christensen for providing us with key magnetic data from the Greenland magnetometer chain. V. Petrov is acknowledged for his contribution in preparing the Viking magnetometer data base. L. Frank, J. Craven and J.S. Murphree kindly prepared the satellite auroral images used in this study. We owe thanks to our colleagues at the Finnish Meteorological institute, H. Koskinen, T. Mäkinen, and M. Mäkelä for pointing out appropriate data and for assisting us in the preparation of the final figures.

#### 5. REFERENCES

1. McPherron R L 1970, Growth phase of magnetospheric substorms, *J Geophys Res*, 75 p. 5592-5599.
2. Untiedt J & al 1978, Observations of the initial development of an auroral and magnetic substorm at magnetic midnight, *J Geophys*, 45, p. 41-65.
3. Pulkkinen T I & al 1991, Auroral signatures of substorm recovery phase: A case study. In: *Magnetospheric Substorms, Geophysical monograph series*, 64, p. 333-341, AGU, Washington.
4. Craven J D & Frank L A 1987, Latitudinal motions of the aurora during substorms, *J Geophys Res*, 92, p. 4565-4573.
5. Opgenoorth H J & al 1992, The recovery phase of magnetospheric substorms and its association with morning sector aurora, to be submitted to *J Geophys Res*.
6. Persson M A L & al 1992, On the difference of ionospheric conductances in the morning and evening sectors of the auroral oval, *Proceedings of the International Conference on Substorms*, ICS-1, Kiruna.
7. Lyons L R & Fennell J F 1986, Characteristics of auroral electron precipitation on the morningside, *J Geophys Res*, 91, p. 11225-11234.
8. Hones E W & al 1986, Detailed observations of the plasma sheet during a substorm on April 24, 1979, *J Geophys Res*, 91, p. 6845-6859.
9. Sergeev V A & al 1990, Average patterns of precipitation and plasma flow in the plasma sheet flux tubes during steady magnetospheric convection, *Planet Space Sci*, 38, p. 355-363.
10. Hultqvist B 1990, The Swedish Satellite Project Viking, *J Geophys Res*, 95, p. 5749.
11. Pellinen R & Kaila K 1991, *Optical ground-based network, Proceedings of the Cluster Workshop*, Svalbard, Norway, 16-19 September 1991 (ESA SP-330).
12. Pellinen R J & al 1990, Satellite and ground-based observations of a fading transpolar arc, *J Geophys Res*, 95, p. 5817-5824.
13. Koskinen H E J & al 1992, Characteristics of pseudo-breakups, *Proceedings of the International Conference on Substorms*, ICS-1, Kiruna.
14. Opgenoorth H J & al 1983, Characteristics of eastward drifting omega bands in the morning sector of the auroral oval, *J Geophys Res*, 88, p. 9171.
15. Pellinen R 1992, How does magnetospheric convection relate to the expansion onset of substorms?, *J Atm Terr Phys*, in press.